SCIENCE CHINA
Physics, Mechanics & Astronomy

• Research Paper •

October 2011 Vol.54 No.10: 1854–1865
doi: 10.1007/s11433-011-4476-9

The dispersion characteristics of the waves propagating in a spinning single-walled carbon nanotube†

CHAN K. T.[1] & ZHAO YaPu[2*]

[1] *Mechanical Engineering Department, The Hong Kong Polytechnic University, Hung Hom, Hong Kong, China;*
[2] *State Key Laboratory of Nonlinear Mechanics (LNM), Institute of Mechanics, Chinese Academy of Sciences, Beijing 100190, China*

Received May 17, 2011; accepted August 3, 2011; published online August 30, 2011

As the nano-motor becomes a mechanical reality, its prototype can be envisaged as nano-sized rotating machinery at a situation, albeit for different purposes, like that in the first half of the 20th century during which rotor dynamics has contributed to boosting machine power capacity. Accordingly, we take the benefit of hindsight to develop a classical framework of vibration analysis. Essentially, the equations of motion are formulated to cope with both the special carbon-nanotube properties and the first author's previously developed spinning beam formalism, establishing a model satisfactorily verified by some available molecular dynamics (MD) data and classical spinning beam results extracted from the literature. The model is inexpensive based on continuum mechanics as an alternative to the less-flexible MD method for simulating wave motion of the spinning single-walled carbon nanotube, yielding several interesting phenomena, including the fall-off and splitting of the wave characteristic curves and the unexpected gyroscopic phase property. Potential applications are proposed.

spinning single-walled carbon nanotube, gyroscopic phase property, nonlocal elasticity, nonlocal Timoshenko beam theory

PACS: 81.07.De, 62.25.+g, 62.30.+d

Nomenclatures

a: CNT length scale
A: cross-sectional area
$\boldsymbol{B}$: CNT eight-coefficient bearing matrix
c_s: shear wave velocity $=\sqrt{\kappa G/\rho}$
c_o: longitudinal wave velocity $=\sqrt{E/\rho}$
$c_{s\alpha}$: phase speed of shear wave in nonlocal Timoshenko beam $=c_s/\sqrt{\alpha'}$
$c_{o\alpha}$: phase speed of longitudinal wave in nonlocal Timoshenko beam $=c_o/\sqrt{\alpha'}$
$\boldsymbol{C}$: bearing damping coefficient matrix
C_{xx}, C_{xy}, C_{yx}, C_{yy}: bearing damping matrix coefficients
$\boldsymbol{C}$: CNT rotor dynamic matrix
e_o: CNT constant
E: Young's modulus
$e^{i\mu}$: phase angular velocity $(\dot{\varphi}_{xo},\dot{\varphi}_{yo})$ relative to spin Ω
$e^{i\theta}$: phase of spin Ω relative to angular velocity $(\dot{\varphi}_{xo},\dot{\varphi}_{yo})$ of cross-section
$F_x(z_{1,2},t), F_x(z_{1,2},t)$: bearing forces in x and y respectively, at location z_1 or z_2
G: shear modulus $=E/2(1+\upsilon)$
h: wall thickness
I: second moment of area
J: rotary inertia $=\rho I$
k: wavenumber (rad/nm)
K: bearing stiffness coefficient matrix
K_{xx}, K_{xy}, K_{yx}, K_{yy}: bearing stiffness matrix coefficients

*Corresponding author (email: yzhao@imech.ac.cn)
†Recommended by Zhao YaPu (Editorial Board Member)

L: length of CNT rotor
m: mass per unit length $= \rho A$
m_α: effective mass at wavenumber k $= m\sqrt{\alpha'} = \rho A\sqrt{\alpha'}$
q: ratio of beam rotation to translation
r_g: radius of gyration $= \sqrt{I/A}$
r: length scale of wave $= c_o r_g / c_s$
t: time (ps)
T_l: kinetic energy of original Timoshenko beam
$T_{\text{trans,nl}}$: nonlocal elasticity-induced translational kinetic energy of nonlocal Timoshenko beam
$T_{\text{rot,nl}}$: nonlocal elasticity-induced rotational kinetic energy of nonlocal Timoshenko beam
$T_{\text{TB-E}}$: total kinetic energy of nonlocal Timoshenko beam $= \mathrm{T}_l + T_{\text{trans,nl}} + T_{\text{rot,nl}} + T_{\text{S}}$
T_S: kinetic energy of beam spin
V: interlayer surface potential, Tersoff-Brenner or Lennard-Jones
$w_x(z_{1,2},t), w_x(z_{1,2},t), \dot{w}_x(z_{1,2},t), \dot{w}_x(z_{1,2},t)$: journal displacements velocities at z_1 or z_2
w_o: arbitrary constant translation amplitude
w_{xo}, w_{yo}: centroidal translation in the respective x_o, y_o axes
$\dot{w}_{xo}$, $\dot{w}_{yo}$: centroidal translational velocities in the respective x_o, y_o axes
x, y, z: fixed (inertial) coordinates (nm)
x_o, y_o, z_o: spinning (floating) coordinates (nm)
z_1, z_2: bearing locations
α': nonlocal k-wave factor $= 1 + \eta^2 k^2$
α: nonlocal elasticity operator $= 1 - \eta^2 \partial_z^2$
η: Eringen's nonlocal parameter $= e_o a$
$\dot{\varphi}_{xo}\varphi_{yo}, \dot{\varphi}_{yo}\varphi_{xo}$: bending projection on spin axis
φ_{xo}, φ_{yo}: cross-sectional bending rotation about the respective x_o, y_o axes
$\dot{\varphi}_{xo}$, $\dot{\varphi}_{yo}$: cross-sectional angular velocities of bending about the respective x_o, y_o axes
γ_{xo}, γ_{yo}: shear deformations about the respective x_o, y_o axes
κ: shear coefficient
λ: wavelength (nm) $= 2\pi/k$
Ω: spinning velocity (rad/ps) and $\Omega' = \dfrac{\Omega}{\omega_{\text{cr}}}$
$\Omega\varphi_{yo}, \Omega\varphi_{yo}$: spin velocity projections in the cross section along respective x_o and y_o axes
ρ: mass per unit volume (density)
υ: Poisson's ratio
ω: wave frequency (rad/ps) and $\omega' = \dfrac{\omega}{\omega_{\text{cr}}}$
ω_{cr}: critical frequency $= c_s/r_g = c_o/r$
$\omega_{\text{cr}\alpha}$: nonlocal critical frequency $= \omega_{\text{cr}}/\sqrt{\alpha'}$
ϖ_{xo}: angular velocity in x_o
ϖ_{yo}: angular velocity in y_o
ϖ_{zo}: angular velocity in z_o axis
$\Box_{s\alpha}^2 \equiv \partial_z^2 - \dfrac{1}{c_s^2}\alpha\partial_t^2$: D'Alembertian for shear wave in nonlocal Timoshenko beam
$\Box_{o\alpha}^2 \equiv \partial_z^2 - \dfrac{1}{c_o^2}\alpha\partial_t^2$: D'Alembertian for longitudinal wave in nonlocal Timoshenko beam
$\partial_t \leftrightarrow (\dot{})$: once time derivative
$\partial_t^2 \leftrightarrow (\ddot{})$: twice time derivative
$\partial_z, \partial_{zo} \leftrightarrow (\,')$: once space derivative
$\partial_z^2, \partial_{zo}^2 \leftrightarrow (\,'')$: twice space derivative

1 Introduction

For the dynamic design of a conceptual nano-sized rotating machine, one has an aim to ascertain its smooth running through avoiding resonances with the force arising from running the shaft system. This justifies our study of the vibration of spinning carbon nanotubes (CNTs), with which a nano-motor has successfully been fabricated [1,2]. Owing to the lattice feature of the CNTs, traditional continuum mechanics is not applicable straightforwardly but the need for a continuum model is obvious especially for a substitution of the more expensive and less-flexible molecular dynamics (MD) model for CNT vibration simulation. There are already some vibration studies in this regard using the so-called Timoshenko beam theory [3–5] and the Eringen's nonlocal elasticity theory [6] where special constitutive relationship has been employed to replace the traditional strain and stress relation, hereafter referred to as the nonlocal Timoshenko beam theory. Hamilton's principle [7,8] and Flügge's shell theory [8,9] are two other approaches, which have resulted in some energy formalisms [7] for our reference. The purposes of these investigations were to understand the effects of tube size, wavenumber, nanotube-lattice length, temperature-induced axial strain, and beam support nature, etc. on the CNT wave and/or vibration characteristics including phase speed, natural frequencies and/or mode shapes [3–5,8–10]. The primary objective was to find data to underlie future design and development of nanoelectromechanical systems (NEMS) devices [10].

The present authors, from the point of view of wave mechanics, consider vibrations of beams as waves in superposition, and have shown that to find the dispersion characteristics of the constituent waves is the essential task [11]. The second task facing us is the way that integrates the nonlocal elasticity (NE) effect into the formulation with the spinning CNT (a nano-sized rotor). For the non-spinning case, Wang and Hu [12] showed that the nonlocal elasticity is an important factor that makes the dispersion characteristics predicted by the nonlocal Timoshenko beam theory consistent with the MD benchmarking scheme, as shown in Figure 1 plotted in normalized form with data extracted from the MD result [12] and from our own spinning nonlocal Timoshenko beam model expressed as eq. (15), taking zero speed as a special case.

Our flexural beam model combines the shear deformation [11–14] and nonlocal elasticity [6] in addition to the gyroscopic effect and the associated helicity properties [14]. So far as a spinning CNT rotor is concerned, this is the first model. Our aim is to provide a better understanding about CNT dynamics to extend its application. In particular, the gyroscopic effect can potentially be used for gauging directions and splitting vibration frequencies.

The rotational nano-motor has become a reality [1] that could see further development due to availability of some millimetre-long CNTs and smooth nano-bearings [2]. Related work [15–17] has already been in progress using atomistic approach, which has put forward a shaft speed limit of 5 rad/ps as a stability criterion and as a reason for a design with the inner nanotube as spinning rotor and with the outer one fixed [17] framing rather like a nano-rotating machinery in similitude of the traditional rotating machines [18,19].

This analogy provides us with a benefit of hindsight that we may proceed to establish a classical framework for design and analysis of the spinning CNT rotor vibration. The present paper is to formulate a mathematical model that represents the vibration of the spinning CNT rotor and to obtain exact expressions for the dispersion characteristics of the waves. MatLab is used to find phase speed (or frequency) versus wavenumber relationships for different rotor speeds with graphical results showing features like divergence, fall-off, wave and frequency splitting and helical structure arising either from the nonlocal elasticity or the gyroscopic effect. The finding of the 90° gyroscopic phase angle between the spin and bending angular velocities is surprising, which is often neglected classically and regarded as zero.

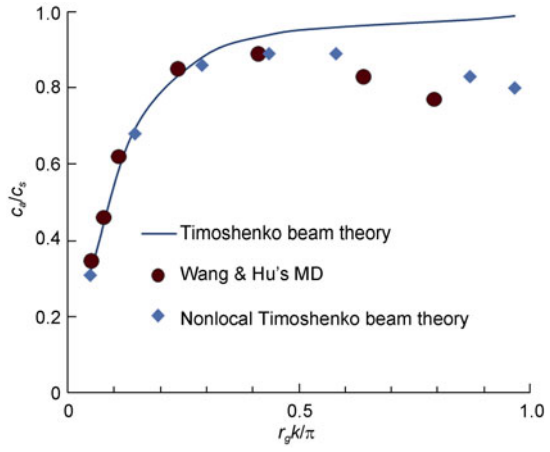

Figure 1 (Color online) Dispersion characteristic of the s_a wave propagating in a CNT modelled by the nonlocal Timoshenko beam theory or the molecular dynamics.

2 The nano-rotating machinery

2.1 Equation of motion of a nano-rotor supported on two bearings

The equation of motion for a CNT rotor in free vibration is written as:

$$\boldsymbol{D}\boldsymbol{s} = \boldsymbol{0}, \tag{1}$$

where $\boldsymbol{0} = \begin{pmatrix} 0 & 0 & 0 & 0 \end{pmatrix}^{\mathrm{T}}$ and $\boldsymbol{s} = \begin{pmatrix} w_x & \varphi_y & w_y & -\varphi_x \end{pmatrix}^{\mathrm{T}}$ is a column matrix with elements representing the translation and rotation displacements. $\boldsymbol{D}$ is an operator containing all the structural information about the spinning CNT. In this conceptual design, the nano-rotating machinery model has the interlayer surface force as supporting bearings to prevent the high speed shaft from contacting the stationary sleeves. The distributed force can be calculated by using suitable energy expressions in refs. [15–17], denoted as V computed using the MD/atomistic simulation, by finding its gradients $-\partial_x V$ & $-\partial_y V$. The localized bearing forces, expressed as a column matrix $\begin{pmatrix} F_x \\ F_y \end{pmatrix}$, are the integrations of $-\partial_x V$ and $-\partial_y V$ over the journal bearing surface. It is related to the shaft local displacement $\begin{pmatrix} w_x \\ w_y \end{pmatrix}$ & velocity $\begin{pmatrix} \dot{w}_x \\ \dot{w}_y \end{pmatrix}$ relative to each bearing sleeve as shown in Appendix A. The eight bearing coefficients in eq. (a1) can be found by employing the classical scheme of Morton [20,21] while using atomistic simulation for computing the forces. Eqs. (a1), (a2) and (1) then yield

$$\{\boldsymbol{D} + [\delta(z - z_1) + \delta(z - z_2)]\boldsymbol{B}\}\boldsymbol{s} = \boldsymbol{0}, \tag{2}$$

where

$$\delta(z - z_1) = \begin{cases} 1 \mapsto z = z_1, \\ 0 \mapsto z \neq z_1, \end{cases} \quad \delta(z - z_2) = \begin{cases} 1 \mapsto z = z_2, \\ 0 \mapsto z \neq z_2, \end{cases}$$

at the two bearing locations. $\boldsymbol{D}$ in eq. (2) is the same as that

in eq. (1). Thus, we may separate the study into two parts: (1) Find $\boldsymbol{D}$ for an indefinitely long CNT rotor as a spinning nonlocal Timoshenko beam on which wave can propagate; (2) find $\boldsymbol{B}$ by computing the eight bearing coefficients, 4 for stiffness $\boldsymbol{K}$ and 4 for damping $\boldsymbol{C}$.

2.2 The kinetic energy expressions and the gyroscopic phase

In the present problem, the gyroscopic and the nonlocal elasticity effect coexist. It is not *in prior* known if there is synergism between them and whether the CNT rotor vibration is in phase with its own spinning momentum. One needs to include these effects in the formulation. With a spinning speed, the CNT is attached to the coordinate system $x_o y_o z_o$, the so-called floating coordinate system [22], which rotates at an angular velocity Ω relative to the right-handed fixed coordinate $x\ y\ z$ system about the z axis in alignment with z_o, as illustrated in Figure 2. In the absence of a wave, the shaft is lying straight along and spinning about the z axis.

From Adali's flexural vibration result [7], we make use of his energy formulations for an extension to a single-walled CNT modelled as a spinning nonlocal Timoshenko beam. The wave function $(w_x \quad \varphi_y \quad w_y \quad -\varphi_x)^{\mathrm{T}}$ transforms to $(\eta w_x' \quad \eta\varphi_y' \quad \eta w_y' \quad -\eta\varphi_x')^{\mathrm{T}}$ for the CNT rotor. Thus, the kinetic energy (KE) expression is

$$T_{\text{TB-E}} = T_{\text{S}} + T_{\text{I}} + T_{\text{trans,nl}} + T_{\text{rot,nl}}, \tag{3}$$

where $T_S = mr_g^2 L\Omega^2/2$ being the energy of the spin of the CNT with length L. T_{I}, $T_{\text{trans,nl}}$ and $T_{\text{rot,nl}}$ are the separated parts of the KE of the CNT rotor expressed as eqs. (b1), (b2) and (b3) of Appendix B, respectively. The total translational and rotational KE are written, respectively, as eqs. (b4) and (b5). The phases $\mathrm{e}^{\mathrm{i}\theta}$ and $\mathrm{e}^{\mathrm{i}\mu}$ appearing in eq. (b5) are the characteristic values to be determined, referred to as the gyroscopic phase. Their physical meaning can be explored in a later section.

2.3 Hamilton's least action principle and the governing equation of motion

Also based on Adali's result [7], we may show that the potential energy (PE) expression for a beam with nonlocal elasticity does not appear to have changed from that of a beam without elasticity. The PE integral for our spinning CNT rotor is written as eq. (b6). The difference between KE and PE is called the Lagrangian L. Its integral with respect to time is called the action S. When the variation δS is

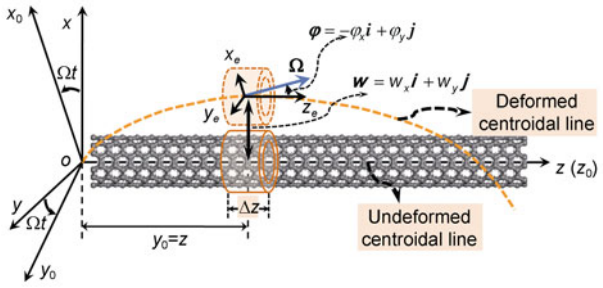

Figure 2 (Color online) Schematic of the coordinate systems of spinning CNT.

zero, the action is least [23]. Hamilton's principle is written as:

$$\delta S = \int_{t1}^{t2} (\delta T_{\text{TB-E}} - \delta V_{\text{TB-E}})\mathrm{d}t = 0, \tag{4}$$

where the complete expressions for $\delta T_{\text{TB-E}}$ and $\delta V_{\text{TB-E}}$ have been derived and given in Appendix B as eqs. (b7) and (b8). Substituting them into eq. (4), after some algebraic procedure, we obtain the governing equation of motion

$$\boldsymbol{D}_o \boldsymbol{s}_o = \boldsymbol{0}, \tag{5}$$

where the matrix elements of $\boldsymbol{D}_o$ are given in Appendix C as eqs. (c1) and (c2) in which the nonlocal operator $\boldsymbol{\alpha} = (1 - \eta^2 \partial_{zo}^2)$ is present. $\boldsymbol{s}_o = (w_{xo} \quad \varphi_{yo} \quad w_{yo} \quad -\varphi_{xo})^{\mathrm{T}}$ is the four-component expression of vibration in terms of translation and rotation as a column matrix, with respect to the floating coordinate system. In Appendix (C), eq. c3) is written for transformation of the coordinate from the floating to the fixed system while eq. (c4) expresses the transformations of the generalized coordinates, translation & rotation respectively. According to Goldstein, similarity transformation [24] is needed to be performed on $\boldsymbol{D}_o$ to complete the so-called invariant transformation to obtain $\boldsymbol{D}$. A simpler method using complex notations can be used as shown in Appendix C, proceeding from eqs. (c5) to resulting in eq. (c10) as the governing equation of motion in the fixed coordinate system. Owing to the physical insight that is implicit through the following analysis, we prefer to give the details in context here as:

$$(\boldsymbol{d} - \mathrm{i}\boldsymbol{g}) \begin{pmatrix} \overline{w} \\ \overline{\phi}^* \end{pmatrix} = \boldsymbol{0}, \tag{6}$$

where $\begin{pmatrix} \overline{w} \\ \overline{\varphi}^* \end{pmatrix} = \begin{pmatrix} w_x + \mathrm{i}w_y \\ \varphi_y - \mathrm{i}\varphi_x \end{pmatrix}$ as in eq. (c5), and

$$\boldsymbol{d} = \begin{pmatrix} \kappa GA\partial_z^2 - m\alpha\partial_t^2 & -\kappa GA\partial_z \\ \kappa GA\partial_z & EI\partial_z^2 - \kappa GA - m\alpha r_g^2 \partial_t^2 + m\alpha r_g^2 (2\mathrm{e}^{\mathrm{i}\theta} - 2\mathrm{e}^{\mathrm{i}\mu} - \mathrm{e}^{2\mathrm{i}\theta} - 1)\Omega^2 \end{pmatrix}, \tag{7}$$

$$\boldsymbol{g}=\begin{pmatrix}0 & 0\\ 0 & -2\Omega m\alpha r_g^2(1-\mathrm{e}^{\mathrm{i}\theta}+\mathrm{e}^{\mathrm{i}\mu})\partial_t\end{pmatrix}. \tag{8}$$

The nonlocal operator is now $\alpha=1-\eta^2\partial_z^2$ referring to z. Eq. (6) is reconverted as eq. (1) with $\boldsymbol{D}=\begin{pmatrix}\boldsymbol{d} & \boldsymbol{g}\\ -\boldsymbol{g} & \boldsymbol{d}\end{pmatrix}$ where the sub-matrices are the same as eqs. (7) and (8). In $\boldsymbol{d}$, $m\alpha r_g^2(2\mathrm{e}^{\mathrm{i}\theta}-2\mathrm{e}^{\mathrm{i}\mu}-\mathrm{e}^{2\mathrm{i}\theta}-1)\Omega^2$ should equal 0 because all centrifugal forces are fictitious according to classical mechanics [23]. In $\boldsymbol{g}$, $(1-\mathrm{e}^{\mathrm{i}\theta}+\mathrm{e}^{\mathrm{i}\mu})$ equals 1 to ensure $2\Omega m\alpha r_g^2(1-\mathrm{e}^{\mathrm{i}\theta}+\mathrm{e}^{\mathrm{i}\mu})\partial_t=2\Omega m\alpha r_g^2\partial_t$ for $\alpha=1$, a correspondence requirement for the CNT rotor dynamics. Given this as a special case, eq. (1) would be the same as eq. (2.3) of Chan et al. [14] or as a similar equation given in Zu and Han [25]. Eq. (6) on the other hand is exactly the same as the equation of motion by Argento and Scott [26]. Thus, one has $\mathrm{e}^{\mathrm{i}\theta}=\mathrm{e}^{\mathrm{i}\mu}=\mathrm{i}$ for the spinning CNT rotor, implying the gyroscopic phase to be a constant angle π/2 irrespective of whether the nonlocal elasticity effect exists or not.

2.4 Interpretation of the gyroscopic phase

The nonzero phase angles, θ & μ, give us a surprise. Classically, gyroscopic top is considered as a rigid body [23] where the phase angles are zero. As a matter of hindsight, however, a spinning CNT beam element is elastic, vibrating at a certain characteristic frequency to produce the apparent precession [14]. The phase, referred to as the gyroscopic phase, can be nonzero. To examine this further from a physical point of view, the angular velocity due to bending is expressed as:

$$\begin{aligned}&(\dot{\varphi}_{xo}\boldsymbol{x}_o+\dot{\varphi}_{yo}\boldsymbol{y}_o)+\mathrm{e}^{\mathrm{i}\theta}\Omega\boldsymbol{z}_o\times(\varphi_{xo}\boldsymbol{x}_o+\varphi_{yo}\boldsymbol{y}_o)\\ &=(\dot{\varphi}_{xo}-\mathrm{e}^{\mathrm{i}\theta}\Omega\varphi_{yo})\boldsymbol{x}_o+(\dot{\varphi}_{yo}+\mathrm{e}^{\mathrm{i}\theta}\Omega\varphi_{xo})\boldsymbol{y}_o,\end{aligned} \tag{9}$$

where the components $-\Omega\varphi_{yo},\Omega\varphi_{xo}$ are the instantaneously projected components of the spin angular velocity onto the beam's cross-section along the respective axes. $\dot{\varphi}_{xo},\dot{\varphi}_{yo}$, are the components of the vibratory angular velocity. Thus, the vibration components are $(\dot{\varphi}_{xo}-\mathrm{i}\Omega\varphi_{yo})$ & $(\dot{\varphi}_{yo}+\mathrm{i}\Omega\varphi_{xo})$ where the imaginary number i comes from $\theta=\pi/2$.

Likewise, the spin angular velocity is expressed as:

$$\begin{aligned}&\Omega\boldsymbol{z}_o+\mathrm{e}^{\mathrm{i}\mu}(\dot{\varphi}_{xo}\boldsymbol{x}_o+\dot{\varphi}_{yo}\boldsymbol{y}_o)\times(\varphi_{xo}\boldsymbol{x}_o+\varphi_{yo}\boldsymbol{y}_o)\\ &=(\Omega+\mathrm{e}^{i\mu}\dot{\varphi}_{xo}\varphi_{yo}-\mathrm{e}^{i\mu}\dot{\varphi}_{yo}\varphi_{xo})\boldsymbol{z}_o,\end{aligned} \tag{10}$$

where $\dot{\varphi}_{xo}\varphi_{yo},\dot{\varphi}_{yo}\varphi_{xo}$ are the projected components of the vibratory angular velocity onto the spin axis, the cause of the spin fluctuation with speed expression as $(\Omega+\mathrm{i}\dot{\varphi}_{xo}\varphi_{yo}-\mathrm{i}\dot{\varphi}_{yo}\varphi_{xo})$. The presence of i is not only natural ($\because\dot{\varphi}_{xo}$ & $\dot{\varphi}_{yo}$ could produce i from differentiation) but also essential for eliminating the fictitious forces from the equation with reference to the fixed coordinate system.

2.5 Wave equation and the helical structure of the waves

Using the wave mechanics approach requires us to consider the wave function $\boldsymbol{s}=\begin{pmatrix}w_x & \varphi_y & w_y & -\varphi_x\end{pmatrix}^{\mathrm{T}}$ as representing a wave entity. By dividing eq. (1) with the constant κGA, one may obtain the wave equation written as:

$$\begin{pmatrix}\partial_z^2-\alpha\partial_t^2/c_s^2 & -\partial_z & 0 & 0\\ \partial_z & r^2(\partial_z^2-\alpha\partial_t^2/c_o^2)-1 & 0 & -(2\Omega/\omega_{\mathrm{cr}\alpha}^2)\partial_t\\ 0 & 0 & \partial_z^2-\alpha\partial_t^2/c_s^2 & -\partial_z\\ 0 & (2\Omega/\omega_{\mathrm{cr}\alpha}^2)\partial_t & \partial_z & r^2(\partial_z^2-\alpha\partial_t^2/c_o^2)-1\end{pmatrix}\boldsymbol{s}=\begin{Bmatrix}0\\0\\0\\0\end{Bmatrix}, \tag{11}$$

where $r=c_o r_g/c_s$ is a length scale, and $\omega_{\mathrm{cr}\alpha}=\omega_{\mathrm{cr}}/\sqrt{\alpha'}$ is the NE critical frequency. The D'Alembertian operators $\partial_z^2-\alpha\partial_t^2/c_s^2$ & $\partial_z^2-\alpha\partial_t^2/c_o^2$ represent the constituent shear and longitudinal waves, respectively. Given the wavenumber k, $\alpha\to\alpha'=1+\eta^2k$ becomes a real number always greater than 1. This in effect means that the speeds of these two constituent waves on the CNT rotor are $c_{s\alpha}=c_s/\sqrt{\alpha'}$ & $c_{o\alpha}=c_o/\sqrt{\alpha'}$. Together with $\omega_{cr\alpha}$, they are reduced from their respective classical values c_s, c_o & ω_{cr} as new constants. Operator α acts on the inertia terms to yield $m_{\alpha}=m\sqrt{\alpha'}=\rho A\sqrt{\alpha'}$ as an increased effective mass.

The wave entity $\boldsymbol{s}$ is helical in structure. One may consider it as a helix traced by its deformed centroidal line with a pitch $\lambda=2\pi/k$ and a revolving speed ω as introduced in Appendix D. Eqs. (d2) and (d3) depict the polarizations [14] as:

$$\begin{aligned}&\phi_1=\arctan(w_y/w_x)=-\omega_1 t+kz\\ &\&\ \phi_2=\arctan(w_y/w_x)=\omega_2 t-kz.\end{aligned} \tag{12}$$

From this equation, one may show that the tip of $\boldsymbol{w}_1$ traces a right-hand (RH) helix and the tip of $\boldsymbol{w}_2$ traces a left-hand (LH) helix. The former revolves anticlockwise (rev-A) at ω_1 rad/s and the latter revolves clockwise (rev-C) at ω_2 rad/s,

both producing a forward wave motion as illustrated in Figures 3(a) and 3(b) for a forward in space (FIS) wave. A scheme exists for finding the revolving standing waves and normal modes based on information about these helical wave properties [14]. The nonlocal elasticity effect does not show explicit influences on the helical geometric structure but implicitly changes the relationship between ω and λ and also alters $q_\alpha = k - \omega^2\alpha'/kc_s^2$, the ratio of the bending angle to the translation.

$$\begin{vmatrix} \alpha'\omega^2/c_s^2 - k^2 & \mathrm{i}k & 0 & 0 \\ -\mathrm{i}k & r^2\alpha'\omega^2/c_o^2 - r^2k^2 - 1 & 0 & -2\mathrm{i}\omega\Omega/\omega_{\mathrm{cr}\alpha}^2 \\ 0 & 0 & \alpha'\omega^2/c_s^2 - k^2 & \mathrm{i}k \\ 0 & 2\mathrm{i}\omega\Omega/\omega_{\mathrm{cr}\alpha}^2 & -\mathrm{i}k & r^2\alpha'\omega^2/c_o^2 - r^2k^2 - 1 \end{vmatrix} = 0. \tag{13}$$

After some algebraic expansion, it becomes a dispersion equation either written as:

$$k^4 - \left(\frac{1}{c_{o\alpha}^2} + \frac{1}{c_{s\alpha}^2}\right)k^2\omega^2 - \frac{1}{c_{o\alpha}^2 r_g^2}\omega^2 + \frac{1}{c_{o\alpha}^2 c_{s\alpha}^2}\omega^4 \pm \frac{2\omega\Omega}{c_{o\alpha}^2}\left(k^2 - \frac{\omega^2}{c_{s\alpha}^2}\right) = 0, \tag{14}$$

or as

$$\left(\frac{c}{c_s}\right)^4 \mp \frac{2\Omega}{\pi\bar{k}\omega_{\mathrm{cr}}}\left(\frac{c}{c_s}\right)^3 - \frac{1}{\alpha'}\left(1 + \frac{c_o^2}{c_s^2} + \frac{1}{\pi^2\bar{k}^2}\right)\left(\frac{c}{c_s}\right)^2 \pm \frac{1}{\alpha'}\frac{2\Omega}{\pi\bar{k}\omega_{\mathrm{cr}}}\left(\frac{c}{c_s}\right) + \frac{1}{\alpha'^2}\frac{c_o^2}{c_s^2} = 0. \tag{15}$$

When $\alpha' = 1$ as a special case, eq. (14) is the same as eq. (2.31) of Chan et al. [14]. Eq. (15) is to express the root $\frac{c}{c_s}$ versus $\bar{k} = \frac{r_g k}{\pi}$. The "+" sign of the 5th term of eq. (14) corresponds to the "–" (& "+") signs of the 2nd (& 5th) terms of eq. (15), representing the rev-A wave. On the other hand, the "–" sign of eq. (14) corresponds to the "+" (& "–") signs of the 2nd (& 5th) terms of eq. (15), representing the rev-C wave. Given Ω positive definite, the sign of c/c_s, as output from the Matlab, becomes an indication: "+" as rev-C while "–" as rev-A solution. From eq. (15), four dispersion curves can be obtained by MatLab to express c/c_s versus $\bar{k}$, taking the following coefficients as input:

$$a_1 = 1, \quad a_2 = -\frac{2\Omega}{\pi\omega_{cr}\bar{k}}, \quad a_3 = -\frac{1}{\alpha'}\left(1 + \frac{c_o^2}{c_s^2} + \frac{1}{\pi^2\bar{k}^2}\right), \quad a_4 = \frac{1}{\alpha'}\frac{2\Omega}{\pi\bar{k}\omega_{cr}} \quad \& \quad a_5 = \frac{1}{\alpha'^2}\frac{c_o^2}{c_s^2}. \tag{16}$$

Eq. (d4) of appendix D has a $\pm$ sign which can be used for differentiating the s_a or s_b [11] wave. For a given $\bar{k}$, we have three cases:

(1) $\omega < \omega_{\mathrm{cr}}/\sqrt{\alpha'}$, taking the "+" sign in eq. (d4) one has the evanescent wave solution; taking "–" sign one obtains the s_a wave solution.

(2) $\omega > \omega_{\mathrm{cr}}/\sqrt{\alpha'}$, taking "+" sign one has the s_b wave

2.6 Phase speed versus wavenumber on the spinning CNT

From eq. (11), the characteristic equation is obtained as:

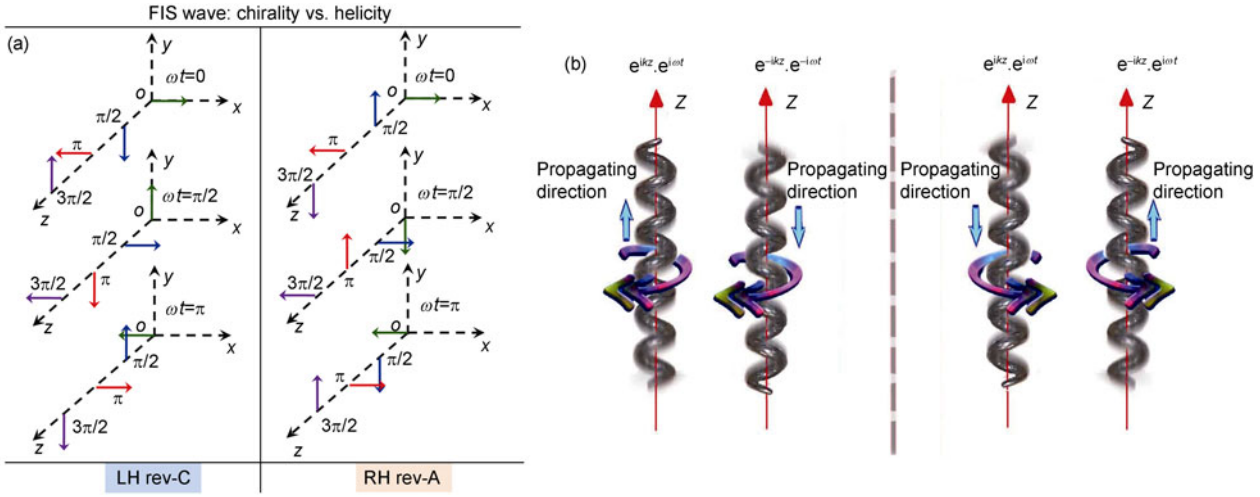

Figure 3 (Color online) Picture of helical waves.

solution, "–" sign the s_a wave solution.

(3) $\omega = \omega_{cr}/\sqrt{\alpha'}$, a thickness shear mode for "+" sign and a s_a wave at that frequency.

A summary is given in table 1.

3 Numerical examples for the Wang, Guo and Hu's armchair (5, 5) CNT

The structural properties of the Wang & Hu's [12] armchair (5, 5) single-walled CNT modelled as a nonlocal Timoshenko beam are:

$$Eh = 346.8 \text{ Pa m}, \quad EI = 1.704\times10^{-26} \text{ Pa m}^4, \quad \upsilon = 0.22,$$
$$r_g = \sqrt{\rho I/\rho A} = 0.152 \text{ nm}, \quad \eta = 0.0355 \text{ nm},$$
$$\rho A = 1.625\times10^{-15} \text{ kg m}^{-1}, \quad \kappa = 0.5,$$
$$\rho h = 760.5 \text{ kg m}^{-3} \text{ nm}, \quad \rho I = 3.736\times10^{-35} \text{ kg m}.$$

Eq. (15) with a α' value has four roots for $\Omega = 0$ as a special case or $\Omega > 0$ as a general case. With the numerical values given, the coefficients (16) as input to MatLab can be calculated for finding the roots to plot c_d/c_s versus $\bar{k}$ as shown in Figure 1. Comparison with the MD data [12] appears to be promising, both models exhibiting a fall-off trend for short wavelength. The two curves agree quite well over the whole wavenumber range, and the continuum model is in good agreement with the MD simulation. We also show the results in Figures 4–6. Based on the above, we make a summary as follows.

4 Summary of the observations

4.1 Fall-off

As shown in Figure 1, the short wave curves exhibit a fall-off trend for both the MD and nonlocal Timoshenko beam models, compared with the classical Timoshenko beam result. This trend is more prominent for the sa wave and does not appear to be markedly affected by the gyroscopic effect, as shown in Figures 4 and 5.

Table 1 MatLab roots identification

Roots $\frac{c}{c_s}$	Type of wave
$> \frac{c_o}{c_s\sqrt{\alpha'}}$	s_b rev-C
$< 1/\sqrt{\alpha'}$	s_a rev-C
$< -\frac{c_o}{c_s\sqrt{\alpha'}}$	s_b rev-A
$0 > \frac{c}{c_s} > -1/\sqrt{\alpha'}$	s_a rev-A

4.2 Divergence trend

As shown in Figure 1, a divergence trend is noticeable at $\bar{k}$ greater than 0.6 indicative of the nonlocal elasticity effect on the shear coefficient κ. Employing Flügge's shell theory [8,9], one may find a more realistic shear coefficient by bridging the gap of the divergence.

4.3 Wave splitting and frequency splitting

Figures 4(a) and 4(b) show respectively the sa and sb dispersion curves, showing that wave splitting arises from the gyroscopic effect. The s_a (s_b) wave splits into a rev-A RH and a rev-C LH revolving helical s_a (s_b) FIS wave. The rev-C wave appears to travel faster than the rev-A wave. Figures 5(a) and 5(b) show the ω versus Ω curves, indicating the frequency splitting due to gyroscopic effect. This is especially marked for the sb wave.

4.4 Non-synergetic mechanisms

Figures 6(a) and 6(b) show that the wave splitting is more marked at lower wavenumbers than at higher wavenumbers, especially for the sb wave. The nonlocal-elasticity fall-off is more predominant at higher wavenumbers, especially for the sa wave. In the intermediate range, both the effects are slight. Thus, the two effects do not appear to constitute a synergism.

The frequency splitting phenomenon can be applied to produce a heterodyning vibration. The heterodyning frequency can be used as a more suitable frequency for measuring the spinning speed of CNT rotor if required because the vibration frequencies themselves may be too high for direct measurement. With a revolving wave, the CNT rotor behaving like a gyroscope can be used to gauge direction. The fall-off phenomenon corresponding to the zero group velocity [27] can be used to produce a vibration energy trap for short-wavelength waves. Since the group velocity governs wave energy transport rate, the gyroscopic effect could allow one to adjust energy transportation through varying the spinning speed. The expression for group velocity $\partial\omega/\partial k$ can be found from equation (D5) by using MatLab.

4.5 A framework for dynamic design of nano-rotor

For the dynamic design of conceptual nano-sized rotating machinery, one has an aim to ascertain its smooth running through avoiding resonances with the force arising from running the rotor system. The initial step is to find the dispersion characteristics for the constituent helical waves on the CNT shaft, based on which the principal normal modes can be found. We may use MatLab and equation (15) to obtain these relationships, c/c_s (or ω) versus k, for the spinning CNT rotor. Given the length and bearing stiffness

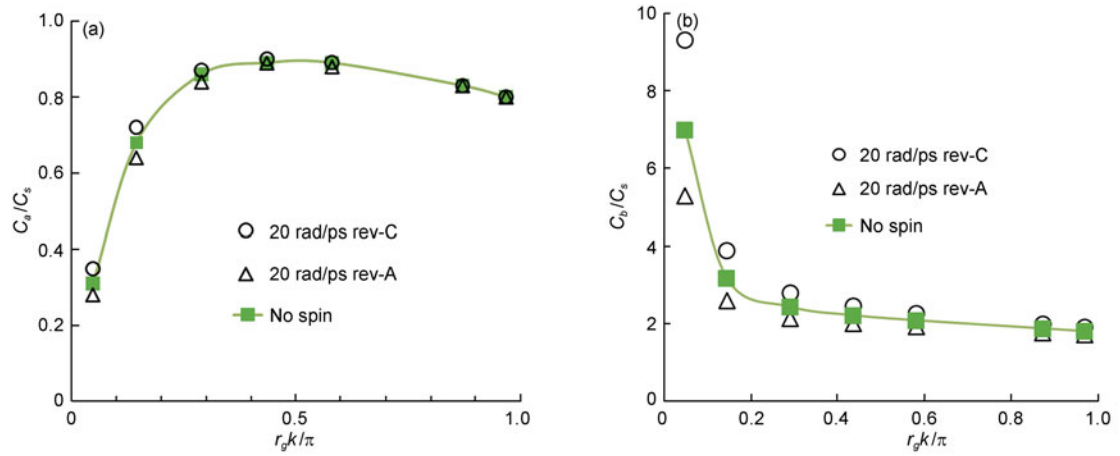

Figure 4 Wave splitting of the s_a (a) and s_b (b) revolving wave propagating in a spinning CNT modelled as a spinning nonlocal Timoshenko beam.

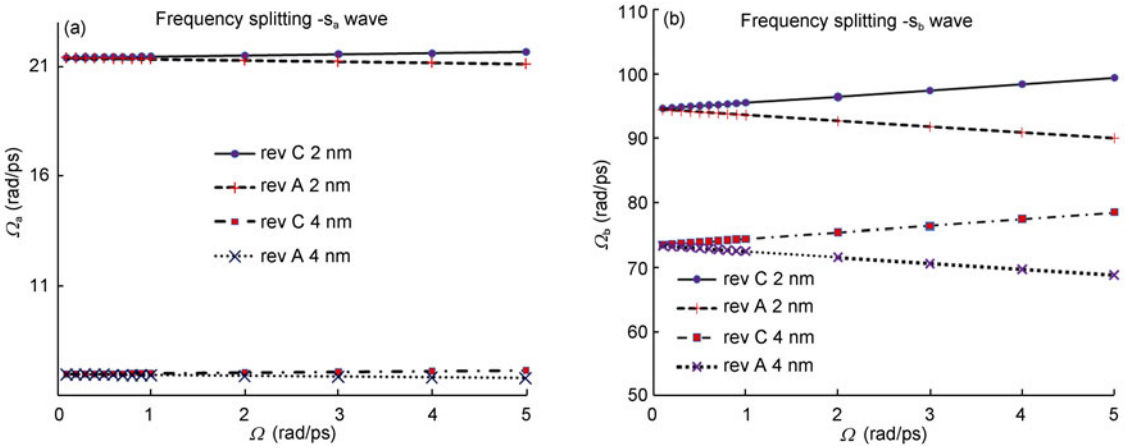

Figure 5 Frequency splitting of the rev C & rev A s_a (a) and s_b (b) waves (wavelengths 2 & 4 nm) propagating in a spinning CNT modelled as a nonlocal Timoshenko beam.

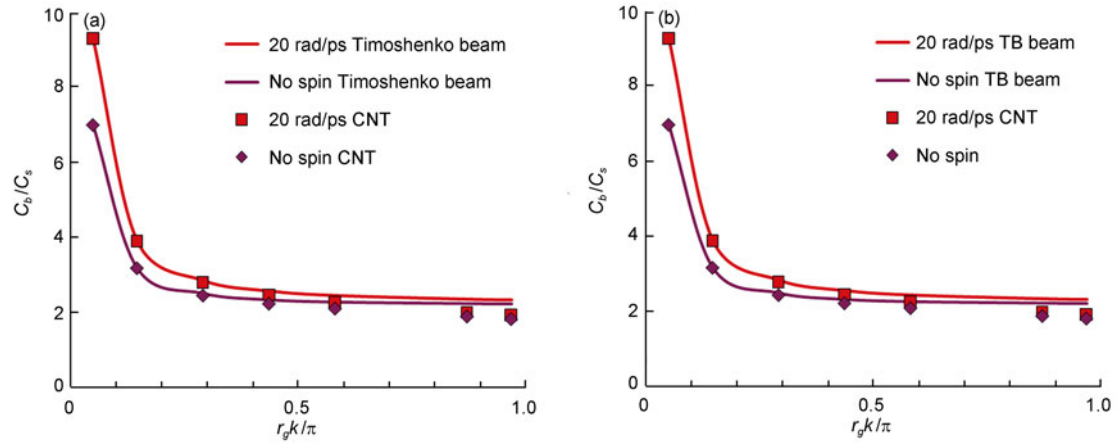

Figure 6 Wave dispersion curves of the rev-C s_a (a) and s_b (b) wave propagating in a CNT modelled as a nonlocal Timoshenko beam with & without spinning compared with the same in a Timoshenko beam.

boundary conditions, the revolving principal normal modes are established using the scheme proposed by Chan et al. [14] (p3921). The normal modes are then used as components in normal mode expansion to represent vibration of the actual CNT rotor with bearing damping and external forces.

Appendix A The bearings and the bearing coefficients

The spinning shaft is elastic and supported on two bearings. It responds to external forces to assume a vibration shape (forced mode shape) with a form depending on how close its running speed is to the natural frequencies [20,21]. The bearings are regarded as consisting of springs and dampers localized at the supporting positions. Their characteristics are modelled using a stiffness and a damping coefficient matrix written as $\boldsymbol{K}=\begin{pmatrix} K_{xx} & K_{xy} \\ K_{yx} & K_{yy} \end{pmatrix}$ and $\boldsymbol{C}=\begin{pmatrix} C_{xx} & C_{xy} \\ C_{yx} & C_{yy} \end{pmatrix}$, respectively. The localized forces [21] at location z_1 or z_2 are expressed as:

$$\begin{Bmatrix} F_x(z_{1,2},t) \\ F_y(z_{1,2},t) \end{Bmatrix} = \boldsymbol{K}\begin{Bmatrix} w_x(z_{1,2},t) \\ w_y(z_{1,2},t) \end{Bmatrix} + \boldsymbol{C}\begin{Bmatrix} \dot{w}_x(z_{1,2},t) \\ \dot{w}_y(z_{1,2},t) \end{Bmatrix}, \tag{a1}$$

where the cross-diagonal elements of $\boldsymbol{K}$ & $\boldsymbol{C}$ couple the motion between the x and y coordinates. Traditional bearings use oil films for lubrication. The eight coefficients of $\boldsymbol{K}$ & $\boldsymbol{C}$ are measured by experiments or calculated based on fluid mechanics theories like using the Reynolds equation [22]. However, the forces at the CNT bearings are due to atomistic potential. Assuming no torques to be generated by the CNT potential, the bearing force is written as

$$\boldsymbol{Bs}=\begin{pmatrix} K_{xx}+C_{xx}\partial_t & 0 & K_{xy}+C_{xy}\partial_t & 0 \\ 0 & 0 & 0 & 0 \\ K_{yx}+C_{yx}\partial_t & 0 & K_{yy}+C_{yy}\partial_t & 0 \\ 0 & 0 & 0 & 0 \end{pmatrix}\begin{Bmatrix} w_x \\ \varphi_y \\ w_y \\ -\varphi_x \end{Bmatrix}. \tag{a2}$$

This force is localized at each bearing support as external force. It is not dependent on the nonlocal elasticity effect.

Appendix B

B.1 Mechanical energy formalism for the CNT rotor

The different parts of KE of the spinning Timoshenko beam are expressed as:

$$T_1=\frac{m}{2}\int_0^L\{r_g^2[\varpi_{xo}^2+\varpi_{yo}^2+\varpi_{zo}^2] + (\dot{w}_{x0}-\Omega w_{y0})^2+(\dot{w}_{y0}+\Omega w_{x0})^2\}\mathrm{d}z_o \tag{b1}$$

with

$$\varpi_{xo}=(\dot{\varphi}_{xo}-\mathrm{e}^{\mathrm{i}\theta}\Omega\varphi_{yo})\boldsymbol{x}_o,\quad \varpi_{yo}=(\dot{\varphi}_{yo}+e^{\mathrm{i}\theta}\Omega\varphi_{xo})\boldsymbol{y}_o \quad \& \quad \varpi_{zo}=(\Omega+\mathrm{e}^{\mathrm{i}\mu}\dot{\varphi}_{xo}\varphi_{yo}-\mathrm{e}^{\mathrm{i}\mu}\dot{\varphi}_{yo}\varphi_{xo})\boldsymbol{z}_o. \tag{b2}$$

$$T_{\mathrm{trans,nl}}=\frac{m}{2}\int_0^L[(\eta\dot{w}'_{x0}-\Omega\eta w'_{y0})^2+(\eta\dot{w}'_{y0}+\Omega\eta w'_{x0})^2]\mathrm{d}z_o \;\&$$

$$T_{\mathrm{rot,nl}}=\frac{mr_g^2}{2}\int_0^L[(\eta\dot{\varphi}'_{xo}-\mathrm{e}^{\mathrm{i}\theta}\Omega\eta\varphi'_{yo})^2+(\eta\dot{\varphi}'_{yo}+\mathrm{e}^{\mathrm{i}\theta}\Omega\eta\varphi'_{xo})^2 + (\Omega+\mathrm{e}^{\mathrm{i}\mu}\eta^2\varphi'_{yo}\dot{\varphi}'_{xo}-\mathrm{e}^{\mathrm{i}\mu}\eta^2\dot{\varphi}'_{yo}\varphi'_{xo})^2]\mathrm{d}z_o. \tag{b3}$$

From these equations, we may group the translational and rotational energies to rewrite

$$\begin{aligned} T_{\mathrm{trans}}+T_{\mathrm{trans,nl}}=&\frac{m}{2}\int_0^L[\dot{w}_{xo}^2+\dot{w}_{yo}^2+\Omega^2(w_{yo}^2+w_{xo}^2) \\ &+2\Omega(\dot{w}_{yo}w_{xo}-\dot{w}_{x0}w_{y0})]\mathrm{d}z_o \\ &+\frac{m}{2}\int_0^L\eta^2[\dot{w}'^2_{xo}+\dot{w}'^2_{yo}+\Omega^2(w'^2_{yo}+w'^2_{xo}) \\ &+2\Omega(\dot{w}'_{yo}w'_{xo}-\dot{w}'_{x0}w'_{y0})]\mathrm{d}z_o, \end{aligned} \tag{b4}$$

$$\begin{aligned} T_{\mathrm{rot}}+T_{\mathrm{rot,nl}}=&\frac{mr_g^2}{2}\int_0^L[\dot{\varphi}_{xo}^2+\dot{\varphi}_{yo}^2+\mathrm{e}^{2\mathrm{i}\theta}\Omega^2(\varphi_{xo}^2+\varphi_{yo}^2) \\ &-2\Omega(\mathrm{e}^{\mathrm{i}\theta}-\mathrm{e}^{i\mu})(\dot{\varphi}_{xo}\varphi_{yo}-\dot{\varphi}_{yo}\varphi_{xo})]\mathrm{d}z_o \\ &+\frac{mr_g^2}{2}\int_0^L\eta^2[\dot{\varphi}'^2_{xo}+\dot{\varphi}'^2_{yo}+\mathrm{e}^{2\mathrm{i}\theta}\Omega^2(\varphi'^2_{xo}+\varphi'^2_{yo}) \\ &-2\Omega(\mathrm{e}^{\mathrm{i}\theta}-\mathrm{e}^{\mathrm{i}\mu})(\dot{\varphi}'_{xo}\varphi'_{yo}-\dot{\varphi}'_{yo}\varphi'_{xo})]\mathrm{d}z_o. \end{aligned} \tag{b5}$$

The phases $\mathrm{e}^{\mathrm{i}\theta}$ and $\mathrm{e}^{\mathrm{i}\mu}$ are determined in the main text.

Strain energy expression for a beam with nonlocal elasticity does not appear to have changed from that of a beam without NE [7], *viz.* $V_{\mathrm{nl}}=V_1$. The NE parameter, η, does not appear in the potential energy (PE) expression. The PE integral is written as:

$$2V_{\mathrm{nl}}=\int_0^L\Big[EI\varphi'^2_{xo}+EI\varphi'^2_{yo}+\kappa GA(w'_{yo}+\varphi_{xo})^2 +\kappa GA(w'_{xo}-\varphi_{yo})^2\Big]\mathrm{d}z_o. \tag{b6}$$

B.2 The variation of kinetic and potential energies

Carrying out integrations by parts, and according to each generalized coordinates, one may group terms to obtain the variations of the KE integrals for the spinning CNT rotor as:

$$\begin{aligned} \int_{t_1}^{t_2}\delta T_{\mathrm{TB\text{-}E}}\mathrm{d}t=&\int_{t_1}^{t_2}(\delta T_{\mathrm{trans}}+\delta T_{\mathrm{rot}}+\delta T_{\mathrm{trans,nl}}+\delta T_{\mathrm{rot,nl}})\mathrm{d}t \\ =&\int_{t_1}^{t_2}\int_0^L m[(-\ddot{w}_{xo}+\Omega^2 w_{xo}+2\Omega\dot{w}_{y0})\delta w_{x0} \\ &+(-\ddot{w}_{yo}+\Omega^2 w_{yo}-2\Omega\dot{w}_{x0})\delta w_{yo}]\mathrm{d}z_o\mathrm{d}t \end{aligned}$$

$$+\int_{t_1}^{t_2}\int_0^L mr_g^2\{[-\ddot{\varphi}_{xo}+\mathrm{e}^{2\mathrm{i}\theta}\Omega^2\varphi_{xo}+2\Omega(\mathrm{e}^{\mathrm{i}\theta}-\mathrm{e}^{i\mu})\dot{\varphi}_{yo}]\delta\varphi_{xo}$$
$$+[-\ddot{\varphi}_{yo}+\mathrm{e}^{2\mathrm{i}\theta}\Omega^2\varphi_{yo}-2\Omega(\mathrm{e}^{\mathrm{i}\theta}-\mathrm{e}^{i\mu})\dot{\varphi}_{xo}]\delta\varphi_{yo}\}\mathrm{d}z_o\mathrm{d}t$$
$$+\eta^2\int_{t_1}^{t_2}\int_0^L m[(\ddot{w}''_{xo}-\Omega^2 w''_{xo}-2\Omega\dot{w}''_{yo})\delta w_{xo}$$
$$+(\ddot{w}''_{yo}-\Omega^2 w''_{yo}+2\Omega\dot{w}''_{xo})\delta w_{yo}]\mathrm{d}z_o\mathrm{d}t$$
$$+\eta^2\int_{t_1}^{t_2}\int_0^L mr_g^2\{[\ddot{\varphi}''_{xo}-\mathrm{e}^{2\mathrm{i}\theta}\Omega^2\varphi''_{xo}-2\Omega(\mathrm{e}^{\mathrm{i}\theta}-\mathrm{e}^{\mathrm{i}\mu})\dot{\varphi}''_{yo}]\delta\varphi_{xo}$$
$$+[\ddot{\varphi}''_{yo}-\mathrm{e}^{2\mathrm{i}\theta}\Omega^2\varphi''_{yo}+2\Omega(\mathrm{e}^{\mathrm{i}\theta}-\mathrm{e}^{\mathrm{i}\mu})\dot{\varphi}''_{xo})\delta\varphi_{yo}]\}\mathrm{d}z_o\mathrm{d}t. \quad (b7)$$

Similarly, we carry out the same procedure as above to obtain the PE integrals as:

$$\int_{t_1}^{t_2}\delta V_{TB-E}\mathrm{d}t=\int_0^L\int_{t_1}^{t_2}[-\kappa GA(w''_{yo}+\varphi'_{xo})\delta w_{yo}$$
$$-\kappa GA(w''_{xo}-\varphi'_{yo})\delta w_{xo}$$
$$+(\kappa GA\varphi_{xo}-EI\varphi''_{xo}+\kappa GAw'_{yo})\delta\varphi_{xo}$$
$$+(\kappa GA\varphi_{yo}-EI\varphi''_{yo}-\kappa GAw'_{xo})\delta\varphi_{yo}]\mathrm{d}t\mathrm{d}z_o. \quad (b8)$$

Hamilton's principle leads to

$$\int_{t_1}^{t_2}\delta T_{\mathrm{TB\text{-}E}}-\delta V_{\mathrm{TB\text{-}E}}\mathrm{d}t=0.$$

Appendix C

C.1 The coordinate transformation and similarity transformation

The sub-matrices of operator $\boldsymbol{D}_o=\begin{pmatrix}\boldsymbol{d}_o & \boldsymbol{g}_o\\ -\boldsymbol{g}_o & \boldsymbol{d}_o\end{pmatrix}$ of eq. (5) are written as:

$$\boldsymbol{g}_o=\begin{pmatrix}2m\alpha\Omega\partial_t & 0\\ 0 & 2mr_g^2\alpha\Omega(\mathrm{e}^{\mathrm{i}\theta}-\mathrm{e}^{\mathrm{i}\mu})\partial_t\end{pmatrix}, \quad (c1)$$

$$\boldsymbol{d}_o=\begin{pmatrix}\kappa GA\partial_{zo}^2-m\alpha\left(\partial_t^2-\Omega^2\right) & -\kappa GA\partial_{zo}\\ \kappa GA\partial_{zo} & EI\partial_{zo}^2-\kappa GA-m\alpha r_g^2\left(\partial_t^2-\mathrm{e}^{2\mathrm{i}\theta}\Omega^2\right)\end{pmatrix}. \quad (c2)$$

The coordinate transformation with $\boldsymbol{R}^{-1}$ is a reverse rotation of the floating plane. It is written in real notations, and in complex notations, is equivalent to $\mathrm{e}^{\mathrm{i}\Omega t}=\cos\Omega t+\mathrm{i}\sin\Omega t$. $\boldsymbol{R}^{-1}$ brings things back to the fixed coordinate system. The transformation from the floating to the fixed coordinate system is written as:

$$\begin{pmatrix}x\\ y\end{pmatrix}=\boldsymbol{R}^{-1}\begin{pmatrix}x_o\\ y_o\end{pmatrix}, \quad (c3)$$

where

$$\boldsymbol{R}=\begin{pmatrix}\cos\Omega t & \sin\Omega t\\ -\sin\Omega t & \cos\Omega t\end{pmatrix}\Rightarrow\boldsymbol{R}^{-1}=\begin{pmatrix}\cos\Omega t & -\sin\Omega t\\ \sin\Omega t & \cos\Omega t\end{pmatrix}.$$

This is accompanied by the transformations of the generalized coordinates (translations & rotations) expressed respectively as:

$$\begin{pmatrix}w_x\\ w_y\end{pmatrix}=\boldsymbol{R}^{-1}\begin{pmatrix}w_{xo}\\ w_{yo}\end{pmatrix}\ \&\ \begin{pmatrix}\varphi_y\\ -\varphi_x\end{pmatrix}=\boldsymbol{R}^{-1}\begin{pmatrix}\varphi_{yo}\\ -\varphi_{xo}\end{pmatrix}. \quad (c4)$$

The negative sign for $-\varphi_{x,\,xo}$ takes the fact that a positive translation in y or y_o will be accompanied by a negative rotation about x or x_o.

C.2 Similarity transformation with complex notations

To complete the transformation, similarity transformation [25] is used on $\boldsymbol{D}_o$. To simplify the mathematical procedure, we use complex notations. The four-component functions become two-component, rewritten as:

$$\begin{pmatrix}\overline{w}_o\\ \overline{\varphi}_o^*\end{pmatrix}=\begin{pmatrix}w_{xo}+\mathrm{i}w_{yo}\\ \varphi_{yo}-\mathrm{i}\varphi_{xo}\end{pmatrix}\ \&\ \begin{pmatrix}\overline{w}\\ \overline{\varphi}^*\end{pmatrix}=\begin{pmatrix}w_x+\mathrm{i}w_y\\ \varphi_y-\mathrm{i}\varphi_x\end{pmatrix}, \quad (c5)$$

where $\mathrm{i}=\sqrt{-1}$. Eq. (5) has two parts: the structural part represented by $\boldsymbol{d}_o$ and the gyro part by $\boldsymbol{g}_o$, written as:

$$\begin{aligned}&\boldsymbol{d}_o\begin{pmatrix}w_{xo}\\ \varphi_{yo}\end{pmatrix}-\mathrm{i}\boldsymbol{g}_o\begin{pmatrix}\mathrm{i}w_{yo}\\ -\mathrm{i}\varphi_{xo}\end{pmatrix}=0\\ \&\ &-\mathrm{i}\boldsymbol{g}_o\begin{pmatrix}w_{xo}\\ \varphi_{yo}\end{pmatrix}+\boldsymbol{d}_o\begin{pmatrix}\mathrm{i}w_{yo}\\ -\mathrm{i}\varphi_{xo}\end{pmatrix}=0.\end{aligned} \quad (c6)$$

Their recombination yields

$$(\boldsymbol{d}_o-\mathrm{i}\boldsymbol{g}_o)\begin{pmatrix}\overline{w}_o\\ \overline{\varphi}_o^*\end{pmatrix}=0, \quad (c7)$$

where

$$(\boldsymbol{d}_o-\mathrm{i}\boldsymbol{g}_o)=\begin{pmatrix}\kappa GA\partial_{zo}^2-m\alpha\partial_t^2-2\mathrm{i}m\alpha\Omega\partial_t+m\alpha\Omega^2 & -\kappa GA\partial_{zo}\\ \kappa GA\partial_{zo} & EI\partial_{zo}^2-\kappa GA-m\alpha r_g^2\partial_t^2+m\alpha r_g^2\mathrm{e}^{2\mathrm{i}\theta}\Omega^2-2\mathrm{i}mr_g^2\alpha\Omega(\mathrm{e}^{\mathrm{i}\theta}-\mathrm{e}^{\mathrm{i}\mu})\partial_t\end{pmatrix}. \quad (c8)$$

dinate system. The similarity transformation is performed to complete the invariant transformation [25] written as:

$$\mathrm{e}^{\mathrm{i}\Omega t}(\boldsymbol{d}_o - \mathrm{i}\boldsymbol{g}_o)\mathrm{e}^{-\mathrm{i}\Omega t}\mathrm{e}^{\mathrm{i}\Omega t}\begin{pmatrix}\overline{w}_o\\ \overline{\varphi}_o^*\end{pmatrix}$$

Thus

$$= \mathrm{e}^{\mathrm{i}\Omega t}(\boldsymbol{d}_o - \mathrm{i}\boldsymbol{g}_o)\mathrm{e}^{-\mathrm{i}\Omega t}\begin{pmatrix}\overline{w}\\ \overline{\varphi}^*\end{pmatrix} = 0. \tag{c9}$$

$$\begin{pmatrix}\kappa GA\partial_z^2 - m\alpha\partial_t^2 & -\kappa GA\partial_z\\ \kappa GA\partial_z & EI\partial_z^2 - \kappa GA - m\alpha r_g^2\partial_t^2 + 2\mathrm{i}\Omega m\alpha r_g^2\left[(1-\mathrm{e}^{\mathrm{i}\theta}+\mathrm{e}^{\mathrm{i}\mu})\partial_t - (1+\mathrm{e}^{2\mathrm{i}\theta}-2\mathrm{e}^{\mathrm{i}\theta}+2\mathrm{e}^{\mathrm{i}\mu})\Omega^2\right]\end{pmatrix}\begin{pmatrix}\overline{w}\\ \overline{\varphi}^*\end{pmatrix} = 0. \tag{c10}$$

Appendix D Helical structure and type of waves

The solutions to eq. (1) for forward in space waves [26] are written as:

$$\begin{pmatrix}w_x\\ \varphi_y\\ w_y\\ -\varphi_x\end{pmatrix} = w_o\begin{pmatrix}1\\ -\mathrm{i}q_\alpha\\ \mathrm{i}\\ q_\alpha\end{pmatrix}\mathrm{e}^{\mathrm{i}(\omega_1 t - kz)}, \tag{d1}$$

$$\begin{pmatrix}w_x\\ \varphi_y\\ w_y\\ -\varphi_x\end{pmatrix} = w_o\begin{pmatrix}1\\ -\mathrm{i}q_\alpha\\ -\mathrm{i}\\ -q_\alpha\end{pmatrix}\mathrm{e}^{\mathrm{i}(\omega_2 t - kz)}.$$

where $q_\alpha = \dfrac{\varphi}{w}$ is the ratio of the bending rotation to the translation. For a specified k, $q_\alpha = k - \dfrac{\omega^2\alpha'}{kc_s^2} = k - \dfrac{\omega^2}{kc_{s\alpha}^2}$. ω_1 or ω_2 is the revolving speed. The transverse displacement vectors from eq. (d1) can be expressed respectively as:

$$\begin{aligned}\boldsymbol{w}_1 &= \mathrm{Re}[\mathrm{e}^{\mathrm{i}(\omega_1 t - kz)}\boldsymbol{e}_x + \mathrm{i}\mathrm{e}^{\mathrm{i}(\omega_1 t - kz)}\boldsymbol{e}_y]w_o\\ &= w_o[\cos(\omega_1 t - kz)\boldsymbol{e}_x - s\sin(\omega_1 t - kz)\boldsymbol{e}_y]\\ &= w_o\boldsymbol{e}\angle\phi_1,\end{aligned} \tag{d2}$$

$$\begin{aligned}\boldsymbol{w}_2 &= \mathrm{Re}[\mathrm{e}^{\mathrm{i}(\omega_2 t - kz)}\boldsymbol{e}_x - \mathrm{i}\mathrm{e}^{\mathrm{i}(\omega_2 t - kz)}\boldsymbol{e}_y]w_o\\ &= w_o[\cos(\omega_2 t - kz)\boldsymbol{e}_x + s\sin(\omega_2 t - kz)\boldsymbol{e}_y]\\ &= w_o\boldsymbol{e}\angle\phi_2.\end{aligned} \tag{d3}$$

Using eqs. (d2) and (d3), the right-hand (RH) anticlockwise (rev-A) and left-hand (LH) clockwise (rev-C) waves can be illustrated in the graphs of figure D(1) below. A propagating wave a can be visualized as a shape like those in the exaggerated photo of figure D(2). From eq. (15), given the pitch, one obtains

$$\left(\frac{c}{c_s}\right) = \sqrt{\frac{\left(1+\dfrac{c_o^2}{c_s^2} - \dfrac{2\Omega}{\omega_{\mathrm{cr}}}\dfrac{1}{\overline{\omega}}\right) \pm \sqrt{\left(1+\dfrac{c_o^2}{c_s^2} - \dfrac{2\Omega}{\omega_{\mathrm{cr}}}\dfrac{1}{\overline{\omega}}\right)^2 - 4\dfrac{c_o^2}{c_s^2}\left(1 - \dfrac{1}{\alpha'\overline{\omega}^2} - \dfrac{2\Omega}{\omega_{\mathrm{cr}}}\dfrac{1}{\overline{\omega}}\right)}}{2\alpha'\left(1 - \dfrac{1}{\alpha'\overline{\omega}^2} - \dfrac{2\Omega}{\omega_{\mathrm{cr}}}\dfrac{1}{\overline{\omega}}\right)}}. \tag{d4}$$

This shows that the wave at a frequency is of two types, one related to the s_a wave and the other to the s_b wave [6]. One may also obtain the relation between ω & k as:

$$\begin{aligned}&\omega'^4 \mp 2\Omega'\omega'^3 - \frac{[(1+r^2)k'^2+1]}{\alpha'}\omega'^2\\ &\pm\frac{2\Omega' k'^2}{\alpha'}\omega' + \frac{k'^4 r^2}{\alpha'^2} = 0.\end{aligned} \tag{d5}$$

The help of Mr. Ting Cai, Mr. K. T. Leung, Drs. Jun Huang, X. Q. Wang, W. O. Wong, Y. Yang and Jin-Liang Zang is acknowledged with thanks. The first author also thanks Professor George Smith for the general discussion concerning the framing of the manuscript. This work was supported by the National Natural Science Foundation of China (Grant Nos. 60936001, 11021262 and 11011120245) and the National Basic Research Program of China (Grant No. 2007CB310500). K. T. C thanks the China Light and Power Company Ltd. for support on work related to turbine generator vibrations.

1 Fennimore A M, Yuzvinsky T D, Han W Q, et al. Rotational actuators based on carbon nanotubes. Nature, 2003, 424: 408–410
2 Kis A, Zettl A. Nanomechanics of carbon nanotubes. Phil Trans R Soc A, 2008, 366: 1592–1611
3 Li X F, Wang B L. Vibrational modes of Timoshenko beams at small scales. Appl Phys Lett, 2009, 94: 101903
4 Bonzair A, Tounsi A, Besseghier A, et al. The thermal effect on vibration of single-walled carbon nanotubes using nonlocal Timoshenko beam theory. J Phys D-Appl Phys, 2008, 41: 225404
5 Wang Q, Varadan V K. Vibration of carbon nanotubes studied using nonlocal continuum mechanics. Smart Mater Struct, 2006, 15: 659–666
6 Eringen A C. On differential equations of nonlocal elasticity and solutions of screw dislocation and surface waves. J Appl Phys, 1983, 54: 4703–4710
7 Adali S. Variational principles for transversely vibrating multiwalled carbon nanotubes based on nonlocal Euler-Bernoulli beam model. Nano Lett, 2009, 9: 1737–1741
8 Usuki T, Yogo K. Beam equations for multi-walled carbon nanotubes derived from Flügge shell theory. Proc R Soc A, 2009, 465: 1199–1226

9 Natsuki T, Ni Q Q. Wave propagation in single- and multi-walled carbon nanotubes filled with fluids. J Appl Phys, 2007, 101: 034319
10 Lu P, Lee H P, Lu C, et al. Dynamic properties of flexural beams using a nonlocal elasticity model. J Appl Phys, 2006, 99: 073510
11 Chan K T, Wang X Q, So R M C, et al. Superposed standing waves in a Timoshenko beam. Proc R Soc A, 2002, 458: 83–108
12 Wang L F, Hu H Y. Flexural wave propagation in single-walled carbon nanotubes. Phys Rev B, 2005, 71: 195412
13 Timoshenko S, Gere J. Mechanics of Material. New York: Van Nostrand Reinhold Company, 1972
14 Chan K T, Stephen N G, Reid S R. Helical structure of the waves propagating in a spinning Timoshenko beam. Proc R Soc A, 2005, 461: 3913–3934
15 Servantie J, Gaspard P. Rotational dynamics and friction in double-walled carbon nanotubes. Phys Rev Lett, 2006, 97: 0606234
16 Zhang S, Liu W K, Ruoff R S. Atomistic simulations of double-walled carbon nanotubes (DWCNTs) as rotational bearings. Nano Lett, 2003, 4: 293–297
17 Huang Z. Coaxial stability of nano-bearings constructed by double-walled carbon nanotubes. Nanotechnology, 2008, 19: 045701
18 Bishop R E D. The vibration of rotating shafts. J Mech Engrg Sci, 1959, 1: 50–65
19 Bishop R E D, Parkinson A G. Vibration and balancing of flexible shafts. Appl Mech Rev, 1968, 21: 439–451
20 Morton P G. Modal balancing of flexible shaft without trial weights. Proc Inst Mech Eng C, 1985, 199: 71–78
21 Morton P G. Measurement of the dynamic characteristics of a large sleeve bearing. Trans ASME J Lubr, 1971, 93: 143–150
22 Choi S H, Pierre C, Ulsoy A G. Consistent modelling of rotating Timoshenko shafts subject to axial loads. J Vib Acous, 1992, 114: 249–259
23 Hand L N, Finch J D. Analytical Mechanics. Cambridge: Cambridge University Press, 1998
24 Goldstein H. Classical Mechanics. 6th ed. Addison-Wesley, 1969
25 Zu J W Z, Han R P S. Natural frequencies and normal modes of a spinning Timoshenko beam with general boundary conditions. J Appl Mech, 1992, 59: S197–S204
26 Argento A, Scott R A. Elastic wave propagation in a Timoshenko beam spinning about its longitudinal axis. Wave Motion, 1995, 21: 67–74
27 Wang L F, Guo W L, Hu H Y. Group velocity of wave propagation in carbon nanotubes. Proc R Soc A, 2008, 464: 1423–1428